Contents lists available at ScienceDirect

Transactions of Nonferrous Metals Society of China

36(2026) 974−987

www.tnmsc.cn

Recovery of valuable metals from lepidolite by hydrochloric acid leaching and kinetics on dissolution of lithium

Song-lin LIU [a], Jin-lian LIU [a,b], Xiao-peng SONG [c], Zhou-lan YIN [b], Xin-hai LI [a,d], Zhi-xing WANG [a,d], Hua-jun GUO [a,d], Guo-chun YAN [a,d], Qi-yang HU [a,c], Xun-hui XIONG [e], Jie-xi WANG [a,c,d*]

[a] School of Metallurgy and Environment, Central South University, Changsha 410083, China;

[b] School of Chemistry and Chemical Engineering, Central South University, Changsha 410083, China;

[c] Jiangxi Yunwei New Materials Co., Ltd., Yichun 330700, China;

[d] National Engineering Research Centre of Advanced Energy Storage Materials, Changsha 410205, China;

[e] School of Environment and Energy, South China University of Technology, Guangzhou 510006, China

Abstract: The leaching process and kinetic behavior of lepidolite in hydrochloric acid were explored systematically. The influence of leaching conditions on the leaching efficiency of valuable metals in lepidolite was investigated. Under optimized conditions, the leaching efficiencies of Li, K, Rb, Cs and Al are 92.02%, 93.31%, 88.59%, 86.75% and 81.07%, respectively. Kinetics research results show that the leaching process conforms to the shrinking core model that is under the mixed control of chemical reaction and diffusion through the solid product layer. In addition, the contribution of solid product layer diffusion to the leaching gradually expands as the temperature rises, but it is still significantly less than the contribution of chemical reaction. Cost saving in the neutralizing agent and leaching processes makes hydrochloric acid an economical leaching agent for lepidolite. Finally, the Li_2CO_3 product with a purity of 99.89% was synthesized from the hydrochloric acid leachate.

Keywords: lepidolite; lithium extraction; hydrochloric acid leaching; kinetics

1 Introduction

Lithium is the lightest metal and exhibits unique physical and chemical properties [1,2]. Lithium chemicals are now widely used in batteries, medicine, lubricants, ceramics, and glass [3−5]. Implementing the global carbon neutrality strategy promotes the continuous development of rechargeable lithium-ion batteries and drives the ever-growing demand and consumption for lithium chemicals [6,7]. As such, the annual growth rate of lithium consumption is expected to be 15% to 30% in the next few decades, and is predicted to reach as high as 1.6×10^6 t of Li_2CO_3 equivalent by 2030 [8,9]. Therefore, it is essential to develop lithium extraction technology to satisfy the demand for lithium consumption.

The identified global lithium resources are 89×10^6 t of Li_2CO_3 based on the latest data from the U.S. Geological Survey (USGS) [9]. The primary lithium resources include surface or underground brine, lithium-bearing hard rock ores and clay minerals [10]. The brine lithium resources account for 78% of the total global lithium resources, and more than 60% of lithium products are extracted from brine lithium due to the lower costs [11,12]. However, as the demand for lithium production continues to expand, lithium-bearing hard rock ores have also become the raw materials for lithium extraction [13]. Brine contains 0.06%−0.15% Li [14],

Corresponding author: *Jie-xi WANG, Tel: +86-731-88836633, E-mail: wangjiexikeen@csu.edu.cn

https://doi.org/10.1016/S1003-6326(25)67010-5

Received 3 July 2024; accepted 4 March 2025

the spodumene $LiAlSi_2O_6$ contains 6.0%−7.5% Li, and lepidolite ($K(Li,Al)_3(Al,Si)_4O_{10}(F,OH)_2$) contains 3.3%−7.74% Li [15−18]. Spodumene has the highest purity of hard rock ores, and lepidolite contains more valuable elements, such as Rb and Cs [19]. Generally, Rb is separated from lepidolite during lithium extraction [20] since it has no independent mineral so far.

The processes for extracting lithium from all types of lithium-bearing solid minerals mainly include pyrometallurgy and hydrometallurgy [21−23]. The primary step of pyrometallurgy is roasting, which causes phase transfer of the minerals to obtain soluble lithium. Then, water or acid leaching is adopted to obtain a lithium-containing leaching solution [13]. The pyrometallurgy is generally divided according to the type of roasting additives, which include sulfuric acid, lime, and sodium/potassium/calcium salts [24,25]. As roasting additives, sodium/potassium/calcium salts can effectively improve the extraction efficiency of rubidium and cesium from lepidolite. The hydrometallurgy is divided into alkaline and acidic leaching processes according to different leaching agents, and it is divided into high-pressure and normal-pressure processes according to various operating conditions [26].

Roasting-leaching and direct acid leaching are the main methods for extracting lithium from minerals. The roasting-leaching process has a high extraction efficiency with short reaction time [27]. The sulfuric acid roasting-leaching is a traditional and typical process for spodumene. It begins with calcining for converting α-spodumene to β-spodumene at 1373 K. Then, the β-spodumene is roasted with an excess of concentrated H_2SO_4 at 473−523 K. Finally, a solution containing lithium sulfate is obtained by water leaching [28]. Although this process is suitable for most lithium-containing minerals, it consumes a large amount of energy with significant sulfur-containing gas emission, which is not in line with policies for achieving global carbon neutrality and environmental protection [29,30].

Direct acid leaching is conducive to extracting valuable elements with low energy consumption from minerals with high amounts of Si and waste rock tailings, and it dramatically reduces the emission of gas pollutants [31−33]. Researchers have studied the sulfuric acid leaching method to extract valuable elements from lepidolite [34]. For lepidolite with a high content of impurities such as Al, Fe, Ca, and F, sulfuric acid leaching will consume a large amount of leaching agent, and the high concentration of residual acid in the leaching solution will expend a mass amount of neutralizing agent [35]. Hydrochloric acid is easy to recycle after leaching due to the easy volatilization of HCl, and it can solve the problem of large acid consumption [26,36,37]. It also reduces the concentration of residual acid in the leaching solution and the burdens of subsequent neutralization processes. However, there are no reports on the direct use of hydrochloric acid to leach various elements from lepidolite and its kinetic characteristics.

In this work, the effect of hydrochloric acid direct leaching on the extraction of valuable elements from lepidolite minerals was studied by optimizing the factors of reaction time, temperature, initial HCl solution concentration, liquid/solid ratio (L/S), and particle size. Through analyzing the influence of the above factors on lithium leaching efficiency, the leaching kinetics of Li from lepidolite was studied using a constrained multiple linear regression analysis method. The economic estimation results of the leaching-neutralization process confirm the advantages of hydrochloric acid as the leaching agent. Finally, a high-purity Li_2CO_3 was synthesized using a multi-step precipitation method, demonstrating the practical application potential of the hydrochloric acid leaching of lepidolite. The element extraction effect from lepidolite by hydrochloric acid and the leaching kinetics of lithium were analyzed, which helped to develop new strategies to process lepidolite minerals.

2 Experimental

2.1 Materials

The raw material lepidolite used in this study was obtained from southern China. It was ground in a ball mill before being used as the samples for the leaching tests. The chemical compositions of the lepidolite are listed in Table 1. The contents of Li, Rb, and Cs in lepidolite are low, and the contents of Si, Al, K and F are high. The phase compositions of the lepidolite are presented in Figs. 1(a) and (b). The raw material contains primarily lepidolite ($K(Li,Al)_3(Al,Si)_4O_{10}(F,OH)_2$), quartz ($SiO_2$) and albite ($NaAlSi_3O_8$). The SEM−EDS results of typical areas in lepidolite as shown in Figs. 1(c) and (d) are

Table 1 Chemical compositions of raw lepidolite (wt.%)

Li	Na	K	Rb	Cs	Al	F	Ca	Si	Fe	Mn	Others
2.12	1.25	6.50	1.21	0.20	14.26	4.46	0.14	23.70	0.13	0.24	45.79

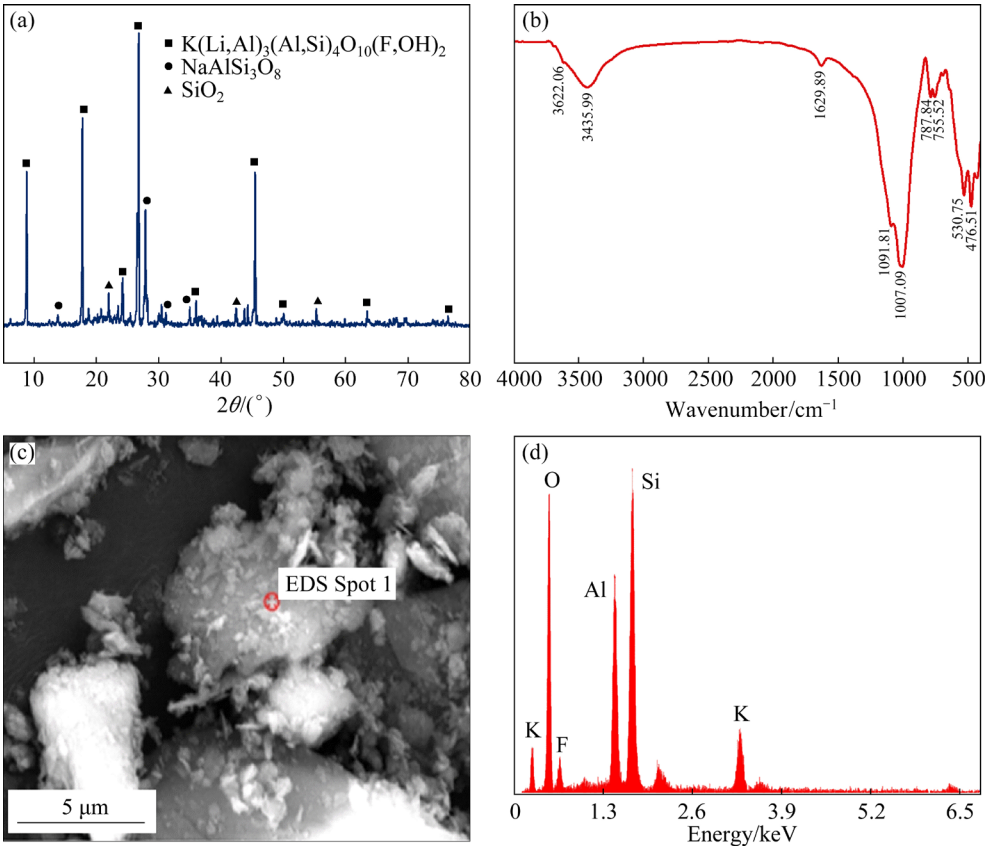

Fig. 1 Characterization results of lepidolite: (a) XRD pattern; (b) FTIR spectrum; (c, d) SEM−EDS results

consistent with the results of the chemical analysis. All chemical reagents used in the experiments are analytical grade, and all solutions are configured with deionized water.

2.2 Experimental procedure

2.2.1 Leaching

The leaching experiment was carried out in a three-neck round bottom flask connected with a condenser pipe and agitated by a mechanical stirrer. The reactor was placed in a constant-temperature oil bath with an automatic temperature control system. All the experiments were conducted in batches with 100 g lepidolite. Firstly, a certain amount of HCl solution with a designed concentration was added to the reactor. Then, the solution was heated under stirring. 100 g of lepidolite was added to the reactor for a leaching reaction when the temperature of the leach solution reached the set value. At certain intervals, 2 mL of the slurry was taken out and filtered to analyze the concentration of elements and calculate the leaching efficiency. A graduated syringe with a filter device was used in the experiment to ensure that the original L/S in the slurry was not changed after sampling. After reaction, the slurry was separated by vacuum filtration, and the leaching residue was dried in an oven at 393 K for 4 h.

2.2.2 Neutralizing and impurities removal

After recovering HCl by evaporation and calcination [26], a NaOH solution with a concentration of 6 mol/L was added to the mother liquor at a dropping speed of 2 mL/min and aged for 60 min at a temperature of 333 K and a stirring speed of 300 r/min for neutralization and impurity removal. Then, a Na_2CO_3 solution with a concentration of 2.12 mol/L was added to the filtrate, and the molar amount of CO_3^{2-} was equal to that of Ca^{2+} in the filtrate. Finally, the Ca-removed solution was obtained by filtrating.

2.2.3 Precipitation of Li_2CO_3

A Na_2CO_3 solution with a concentration of 2.12 mol/L was firstly placed in the reactor and heated to 368 K. Then, the above-mentioned Ca-removed solution was added at a rate of 5 mL/min. After controlling the equimolar amount of Na and Li, the solution was aged for 60 min. Finally, the residue was washed three times with ultrapure water in countercurrent flow, and dried in an oven at 393 K for 2 h.

2.3 Characterization

The powder X-ray diffraction (XRD, Empyrean 2) using Cu K_α radiation was employed to identify the crystalline phase of the samples. The microstructure and element distribution of the samples were examined by scanning electron microscope (SEM, JSM−7900F) coupled with energy-dispersive X-ray spectroscope (EDS). The analyses of metal ions in the digesting solution of solid phase products and leaching solution at different purification stages were carried out by an inductively coupled plasma (ICP, ICAP7400radial). The determination of F in lepidolite, intermediate solid, and liquid samples was conducted by using the fluoride ion selective electrode. The particle size distribution of solid samples was characterized by a laser particle size analyzer (Mastersizer 3000). The structure of samples was tested using the Fourier transform infrared spectrometer (FTIR, Nicolet iS50).

2.4 Analytical methods

All element contents were tested three times using the corresponding method, and the average value was obtained, with the relative standard error within ±0.5%. The leaching efficiency of valuable elements was calculated according to Eq. (1) (taking Li as an example) [38]:

$$X_{\mathrm{Li}}=\frac{\left(V_0-\sum_{i}^{i-1}V_i\right)w_{\mathrm{Li},i}+\sum_{i}^{i-1}V_i w_{\mathrm{Li},i}}{m w_{\mathrm{Li}}}\times 100\% \quad (1)$$

where X_{Li} is the leaching efficiency of lithium (%), V_0 is the initial volume of the leaching solution (L), V_i is the volume of sample solution i (L), w_{Li} is the content of lithium in the lepidolite (dried solid, mass fraction, %), $w_{\mathrm{Li},i}$ is the concentration of lithium in sample i (g/L), and m is the initial mass of lepidolite (g, dried solid).

3 Results and discussion

3.1 Chemical reactions during leaching process

Researchers have explored the dissolution mechanism of lepidolite in sulfuric acid. During the sulfuric acid leaching process, lepidolite is only partially dissolved and reacts with sulfuric acid to form alkali metal sulfate and aluminum sulfate. The contents of alkali metal and aluminum in the residue are low. Trace amounts of Fe and Mn in the mineral are dissolved in the leaching solution. This result has little impact on the acid consumption of the leaching solution, the leaching efficiency of valuable elements, the concentration of lithium in the leaching solution, and the composition of the product. The reaction of lepidolite and hydrochloric acid will form soluble chlorides, making lepidolite more easily dissolved. As such, the valuable metals can be recovered effectively from minerals. For alkali metals and Al, the possible reactions are Reactions (2) and (3) [26]. Since iron, manganese, and calcium exist in lepidolite, the possible reactions are shown in Reaction (4). Therefore, quartz and feldspar are the main components of the leaching residue after the complete erosion of lepidolite by HCl solution.

$$Me_2O\ (s)+2HCl\ (aq)=2MeCl\ (aq)+H_2O\ (l)\ (Me=\text{alkali metals}) \quad (2)$$

$$Al_2O_3\ (s)+6HCl\ (aq)=2AlCl_3\ (aq)+3H_2O\ (l) \quad (3)$$

$$(Fe,Mn,Ca)O\ (s)+2HCl\ (aq)=(Fe,Mn,Ca)Cl_2\ (aq)+H_2O\ (l) \quad (4)$$

3.2 Effect of experimental parameters on leaching process

Both alkali metals and Al can be dissolved in the hydrochloric acid leaching solution, so the leaching efficiencies of these metals reflect the extent of mineral leaching. The effects of leaching time, temperature, initial HCl concentration (c_{HCl}), L/S (mass ratio) and mineral particle size (d_{50}) on the leaching efficiencies of these metals were systematically studied. The change in the leaching efficiency of valuable elements in lepidolite with time is shown in Fig. 2(a). When the reaction time extends from 2 to 4 h, the leaching efficiency of Li increases from 77.32% to 92.02%, and continues to grow to 94.18% at a time extended to 6 h. The changing trends of the leaching efficiencies of K, Rb, and Cs with time are similar to that of Li. When the

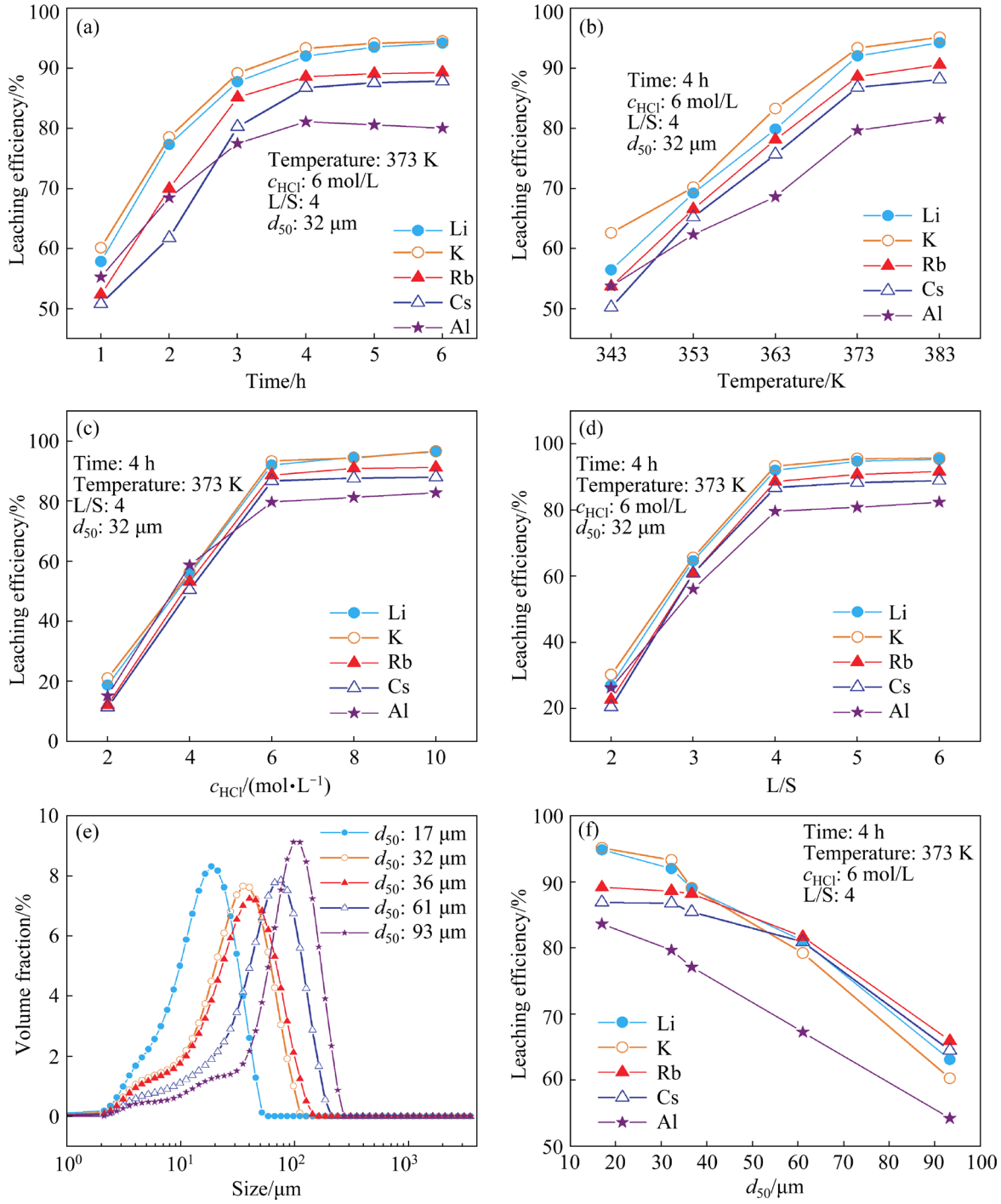

Fig. 2 Effect of various experimental parameters on leaching efficiencies of alkali metals and Al from lepidolite: (a) Leaching time; (b) Leaching temperature; (c) Initial HCl concentration; (d) L/S; (e) Particle size distribution of lepidolite raw materials; (f) Mineral particle size

reaction reaches 6 h, the leaching efficiencies of metals no longer increase significantly, and most of the lepidolite is dissolved. In particular, the leaching efficiency of Al tends to decrease after 4 h of reaction because Al and F can form a stable Al−F complex [26]. Considering the energy consumption and production efficiency issues caused by extending the time, the preferred leaching time here is 4 h.

As shown in Fig. 2(b), the leaching efficiency of valuable elements in lepidolite increases significantly with increasing temperature. When the temperature increases from 343 to 373 K, the leaching efficiency of Li rises from 56.39% to 92.02%. However, the leaching efficiency of Li only increases by 2.19% when the temperature continues to increase to 383 K, and the increase rate of the

leaching efficiency of other elements also slows down. HCl solution is easy to volatilize during high-temperature reaction. Considering energy, equipment investment and operating environment, the preferred reaction temperature here is 373 K.

As shown in Fig. 2(c), the leaching efficiency of valuable elements increases significantly with the increase of initial HCl concentration from 2 to 6 mol/L. When the concentration continues to increase, the leaching efficiency no longer increases significantly. When the acid concentration is 2 mol/L, the leaching efficiency of metals is around 20% due to the lack of acid in the slurry. More H^+ participates in the surface diffusion of the leaching process as the initial HCl concentration increases, thereby increasing the leaching efficiency of valuable elements in lepidolite. Although the leaching efficiency of Li reaches 96.42% when the initial HCl concentration is 10 mol/L, the preferred initial HCl concentration here is chosen as 6 mol/L because the HCl solution is volatile and corrosive.

The leaching efficiency of valuable elements during the leaching process of lepidolite changes with the L/S. As shown in Fig. 2(d), when the L/S increases from 2 to 4, the leaching efficiency of Li increases from 26.96% to 92.02%. When the L/S is between 4 and 6, it has little effect on the leaching efficiency of valuable elements. The effect of L/S on the reaction is consistent with that of initial HCl concentration, because both affect the total amount of acid in the slurry that can be used for leaching reaction. The L/S greater than 4 will cause problems such as increased material flow, low concentration of components in the leaching solution, and large consumption of leaching agents. Therefore, the preferred L/S here is 4.

According to the particle size, lepidolite is divided into five parts by passing through the sieves with different standard aperture sizes. The size distribution of the five parts detected by laser particle size analyzer is shown in Fig. 2(e), where d_{50} is 17, 32, 36, 61 and 93 μm, respectively. The effects of mineral particle size on the leaching efficiencies of valuable elements are studied over the d_{50} range from 17 to 93 μm. As shown in Fig. 2(f), when d_{50} of lepidolite is from 32 to 93 μm, the leaching efficiency of valuable elements gradually increases as the particle size shrinks. The leaching efficiency of Li is 63.08% and 94.83% when d_{50} of lepidolite is 93 and 17 μm, respectively. The particle size dramatically influences the leaching behavior of valuable elements in lepidolite. Reduced particle size means increased mechanical grinding of lepidolite, which will enhance the degree of peeling and disintegration of lepidolite and feldspar, increasing the reactivity of raw materials and the contact area between the leaching agent and mineral particles [39]. At the same time, the fine particles are conducive to shortening the distance for the products to diffuse into the solution and strengthening the dissolution of lepidolite. Considering the energy consumption of ball milling for particle refining, the optimized mineral particle is considered as d_{50}=32 μm.

3.3 Physicochemical properties of leaching residue

The optimized experimental conditions are determined to be the leaching time of 4 h, the temperature of 373 K, the initial HCl concentration of 6 mol/L, the L/S of 4, and the mineral particle size d_{50} of 32 μm. In such conditions, the leaching efficiencies of Li, K, Rb, Cs and Al are 92.02%, 93.31%, 88.59%, 86.75% and 73.84%, respectively. The main components of leaching residue are Si, Al, F and Na, while the contents of Li, K, Rb, and Cs are low (Table 2).

The phase composition of the leaching residue is lepidolite, albite and quartz, which is consistent with the chemical composition (see Fig. 3(a)). In addition, the intensity of the characteristic peak representing SiO_2 is low, indicating that SiO_2 present in the leaching residue is an amorphous phase. The lepidolite phase in the leaching residue is still the primary phase, indicating that the crystal structure of lepidolite in the mineral is not entirely destroyed during the hydrochloric acid leaching process [32,40,41]. During leaching, lepidolite is converted into amorphous SiO_2 and soluble salts. The main composition of leaching residue is SiO_2, accompanied by a small amount of incompletely reacted lepidolite and albite. It can be seen that after leaching with HCl solution, the stretching vibration absorption peak of lepidolite near 3622.06 cm^{-1} (Fig. 1(b)) that is attributed to the O—H group has disappeared (Fig. 3(b)). The two absorption peaks of lepidolite at 755.52 and 787.84 cm^{-1} merge into one absorption peak near 796.91 cm^{-1} after leaching due to the degenerate stretching vibration of the [SiO_4] group [42]. It remains a fact that Al is able to split

Table 2 Chemical compositions of leaching residue (wt.%)

Li	Na	K	Rb	Cs	Al	F	Ca	Si	Fe	Mn	Others
0.26	1.16	0.30	0.01	<0.01	3.53	2.27	<0.01	48.83	<0.01	<0.01	43.64

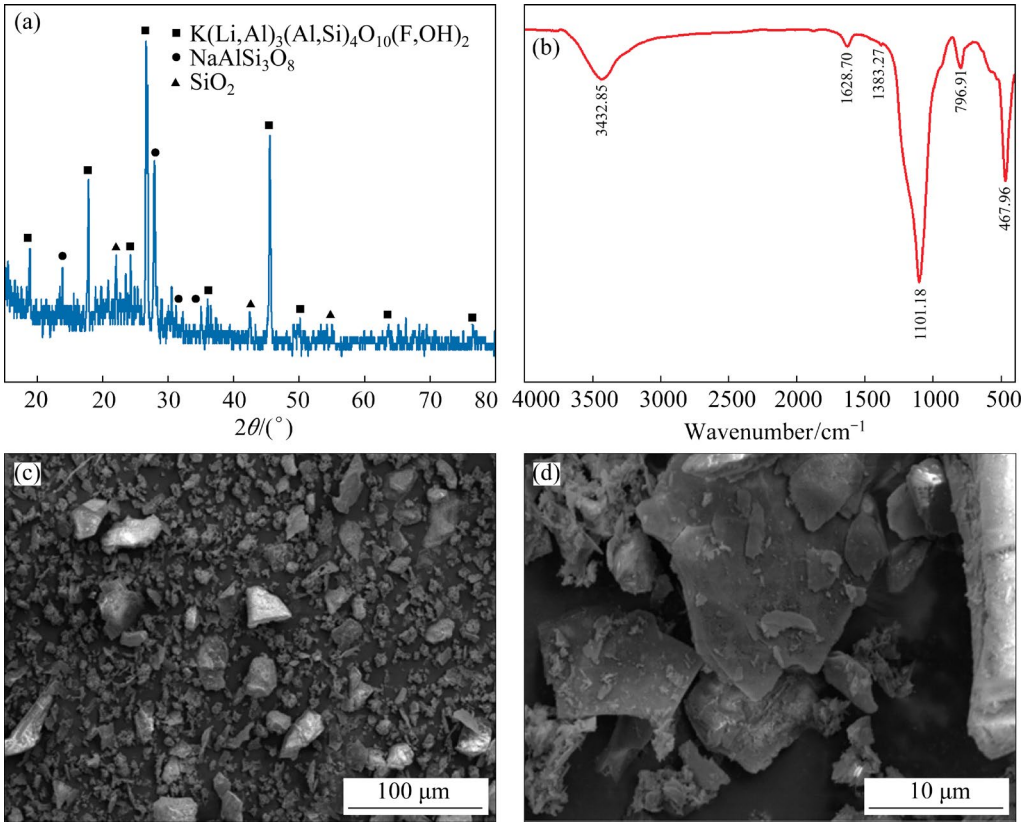

Fig. 3 Characterization results of leaching residue: (a) XRD pattern; (b) FTIR spectrum; (c, d) SEM images

the Si—O bending vibration. Therefore, after Al leaching, the absorption peaks at 476.51 and 530.75 cm^{-1} in the low-frequency region degenerate into an absorption peak near 467.96 cm^{-1}. As shown in Figs. 3(c) and (d), there are many sporadic debris particles in the leaching residue, and the particles are uneven, irregular, and small-sized blocks.

3.4 Kinetics analysis results

The Kinetics models reflect comprehensive information about the leaching mechanism. In the solid−liquid reaction, lepidolite mineral particles are regarded as non-porous particles. During the leaching process of valuable elements, the mineral particles gradually shrink and form a product layer around the unreacted mineral particles, while the shape and size of the particles do not change. When hydrochloric acid is far in excess, it can be considered that the concentration of acid remains unchanged during the reaction. The reaction of hydrochloric acid leaching process is a non-catalytic heterogeneous reaction. Therefore, the shrinking core model (SCM) is used to explain the kinetics here [43,44].

Research results on the SCM model show that three main mechanisms, i.e. liquid film diffusion, solid product layer diffusion and chemical reaction, affect leaching kinetics. If one of the above mechanisms is significantly slower than the other two steps, that step becomes the controlling step in the leaching process. The relevant equations for different control mechanisms are as follows [43,45]:

Liquid film diffusion control:

$$t/\tau_F = x \tag{5}$$

$$\frac{t-t_1}{\tau_F} = x - x_1 \tag{6}$$

Solid product layer diffusion control:

$$\frac{t}{\tau_P} = 1 - 3(1-x)^{2/3} + 2(1-x) \tag{7}$$

$$\frac{t-t_1}{\tau_P} = 3[(1-x_1)^{2/3} - (1-x)^{2/3}] - 2(x-x_1) \tag{8}$$

Chemical reaction control:

$$\frac{t}{\tau_R}=1-(1-x)^{1/3} \tag{9}$$

$$\frac{t-t_1}{\tau_R}=(1-x_1)^{1/3}-(1-x)^{1/3} \tag{10}$$

where t is the real leaching time, t_1 is the time at the change in the rate-controlling step, x is the leaching efficiency of Li, x_1 is the leaching efficiency of Li at t_1, and τ_F, τ_P and τ_R are the time constants of completion of leaching in liquid film diffusion control, solid product layer diffusion control and chemical reaction control, respectively (contribution of each mechanism in the time of complete dissolution of particles).

According to Eqs. (5), (7) and (9), when a contain step is the rate controlling step, a plot of x, $1-3(1-x)^{2/3}+2(1-x)$ and $1-(1-x)^{1/3}$ versus time is a straight line with a slope of $1/\tau_F$, $1/\tau_P$ and $1/\tau_R$, respectively. To determine the control step of the leaching process and conduct kinetics analysis, the changes in leaching efficiency with time under different experimental conditions were analyzed. As shown in Fig. 4, increasing the temperature, initial HCl concentration and L/S and reducing the mineral particle size are beneficial to improving the leaching efficiency of Li.

The leaching efficiency data are substituted into Eqs. (5), (7) and (9) for calculation, and the results are shown in Figs. 5(a−c), respectively. The dependence of results and the kinetics equation is evaluated with the correlation coefficient (R^2) values, and the slope of the fitted line is defined as the rate constant (k_r). The results indicate that the straight lines of Figs. 5(a) and (c) have an obvious inflexion point at 20 min, which often means that a change in the rate-control mechanism has occurred at this time [43,46]. It is worth noting that the straight lines in Fig. 5(b) have linearity within 0−120 min, indicating that the solid product layer diffusion is one of the steps controlling the leaching reaction rate in this time region. The main component of the solid product layer is unreacted SiO_2 [26], silica lepidolite and albite (Table 2 and Fig. 3). The apparent activation energy (E_a) is determined using the slopes of all straight lines in Fig. 5(b) based on the Arrhenius equation:

$$\ln k_r=\ln A-\frac{E_a}{RT} \tag{11}$$

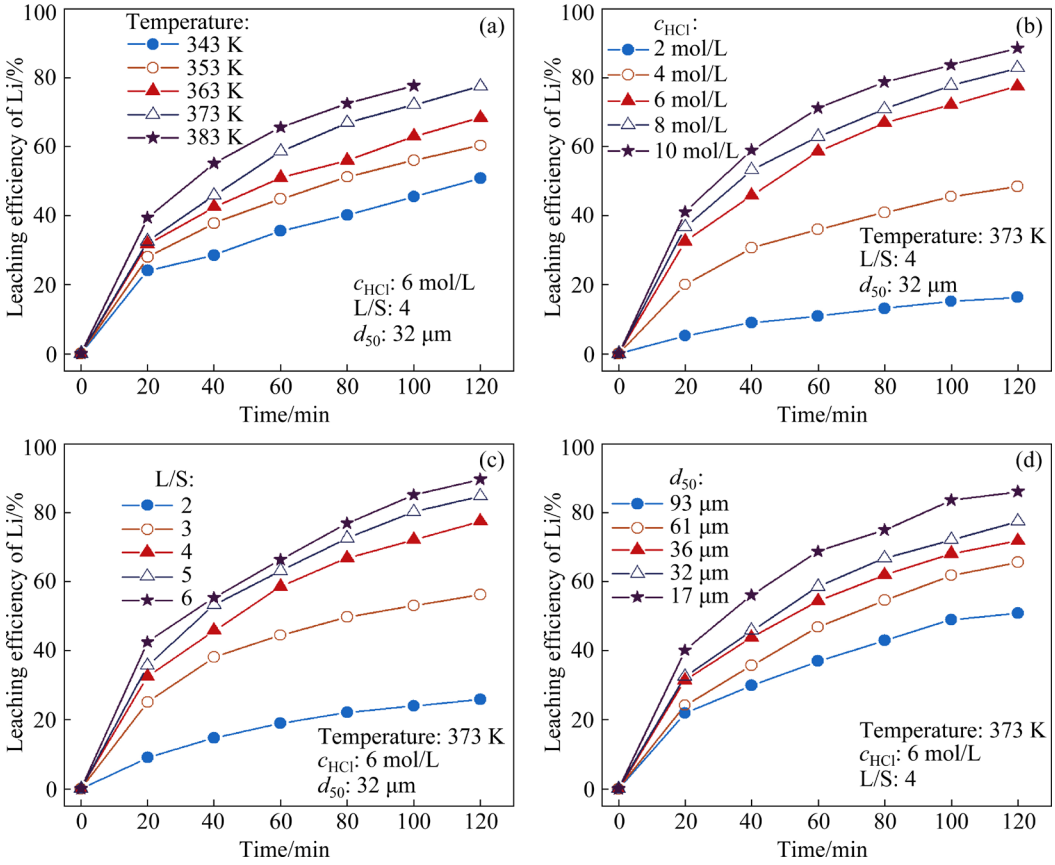

Fig. 4 Leaching efficiency of Li versus time under different leaching conditions

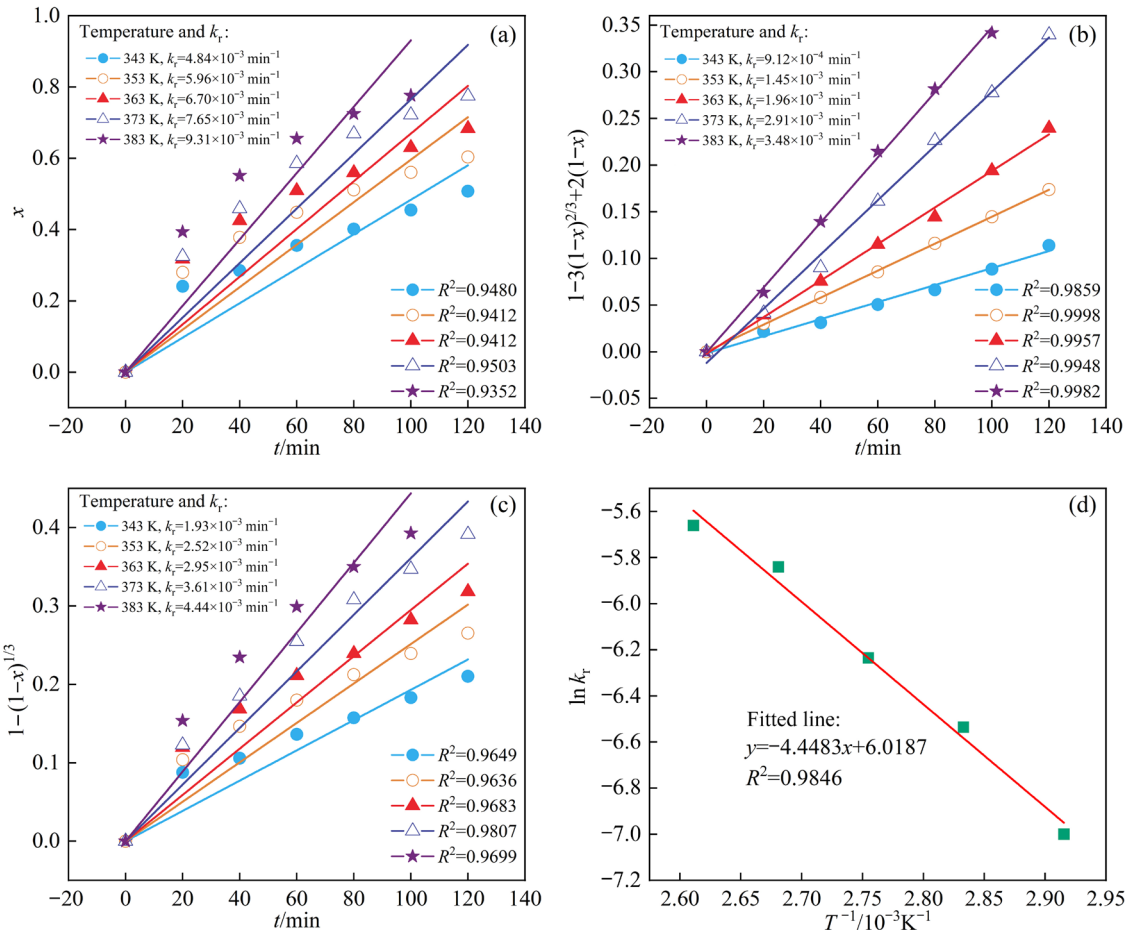

Fig. 5 Plots of x vs t (a), $1-3(1-x)^{2/3}+2(1-x)$ vs t (b), $1-(1-x)^{1/3}$ vs t (c) at different temperatures within 0−120 min, and Arrhenius plot (d) for Li leaching (c_{HCl}: 6 mol/L; L/S: 4; d_{50}: 32 μm)

where A is the pre-exponential factor, R is the molar gas constant (8.314 J/(mol·K)), and T is the thermodynamic temperature.

Arrhenius plot of ln k_r vs T^{-1} for leaching data of Li is shown in Fig. 5(d). The apparent activation energy (E_a) calculated from the slope of the line is 36.983 kJ/mol at 343−383 K. According to previous kinetics studies [47,48], when the apparent activation energy is between 20 and 40 kJ/mol, it often means that the reaction is controlled by mixing steps. The results show that solid product layer diffusion is just one of the influence factors of the leaching reaction. Since the control mechanism of the leaching reaction rate changes at 20 min, it is necessary to explore the kinetics characteristics of the leaching reaction starting from 20 min [49]. The leaching reaction may be controlled by mixed liquid film diffusion, solid product layer diffusion and chemical reaction. Therefore, 20 min was selected as a starting point for calculating the weight of different independent control steps using the following generalized formulas [43,45,50]:

$$t-t_1=\tau_F(x-x_1)+\tau_P[3(1-x_1)^{2/3}-3(1-x)^{2/3}-2(x-x_1)]+\tau_R[(1-x_1)^{1/3}-(1-x)^{1/3}] \quad (12)$$

$$k_r(t-t_1)=B[3(1-x_1)^{2/3}-3(1-x)^{2/3}-2(x-x_1)]+(1-x_1)^{1/3}-(1-x)^{1/3} \quad (13)$$

$$\tau_F=\frac{\rho_B r_0(1-x_1)^{1/3}}{3bk_cC_A} \quad (14)$$

$$\tau_P=\frac{\rho_B r_0^2(1-x_1)^{2/3}}{6bD_eC_A} \quad (15)$$

$$\tau_R=\frac{\rho_B r_0(1-x_1)^{1/3}}{bk_RC_A} \quad (16)$$

where x_1 is the leaching efficiency of Li at 20 min, t_1 is the time (20 min) of the change in the rate-controlling step, C_A is the HCl concentration, b is the stoichiometric coefficient for mineral, k_c is the mass transfer coefficient in the liquid film, D_e is the effective diffusivity of the leaching agent in the product layer, k_R is the reaction rate constant, B is the

constant related to temperature, ρ_B is the molar density of the reactive component in the solid, and r_0 is the initial radius of the particle. The contribution of the above three mechanisms can be estimated based on the values of τ_F, τ_P and τ_R. Under the constraints that τ_F, τ_P and $\tau_R \geq 0$, the values of τ_F, τ_P and τ_R are determined by minimizing the value of φ in the following optimization equation:

$$\varphi=\sum\left\{\tau_F(x-x_1)+\tau_P[3(1-x_1)^{2/3}-3(1-x)^{2/3}-2(x-x_1)]+\tau_R[(1-x_1)^{1/3}-(1-x)^{1/3}]-(t-t_1)\right\}^2 \quad (17)$$

Equation (17) is fitted using multiple linear regression analysis, and the results are listed in Table 3. The results show that, the τ_F is equal to zero at a reaction time of 20−120 min, meaning that the liquid film diffusion does not affect the leaching efficiency of Li. Therefore, the leaching data can be substituted into Eq. (13) for linear fitting to solve for k_r, where B is calculated using τ_P/τ_R [43]. The τ_R/τ_P ratio gradually decreases as the temperature increases, but the τ_R is still significantly greater than τ_P. This indicates that the impact of solid product layer diffusion on the leaching efficiency of Li gradually increases as the temperature rises, but its influence is always less than that of chemical reaction. This is different from the kinetic characteristics when sulfuric acid is used as the leaching agent [34]. It is worth noting that the time constants to complete the reaction increase at 383 K. This is due to the change in the concentration of leaching agent caused by the massive volatilization of HCl at 383 K.

Table 3 τ_F, τ_P and τ_R calculated from leaching data of Li and minimizing value of φ in Eq. (17)

Temperature/K	τ_F	τ_P	τ_R	τ_R/τ_P ratio ($1/B$)	R^2
343	0	0.6277	569.1100	906.66	0.9985
353	0	0.5635	406.8556	722.02	0.9958
363	0	0.5382	349.7612	649.89	0.9976
373	0	0.5012	283.8909	566.42	0.9941
383	0	0.5771	305.9568	530.16	0.9919

Equations (13) and (11) are used to fit the experimental data, and the results are shown in Figs. 6(a) and (b), respectively. The apparent activation energy (E_a) calculated from the slope of the line is 26.765 kJ/mol at 343−373 K. This is consistent with the conclusion mentioned above that the lithium leaching reaction is affected by both the chemical reaction and the solid product layer diffusion within 20−120 min [51]. There is a significant difference in the apparent activation energy of the reaction calculated based on the reaction time of 0 and 20 min, which indicates that changes in the chemical reaction occur during the leaching of lepidolite in hydrochloric acid. It means that various lithium-containing minerals with different reactivities are embedded in lepidolite [29,49]. The results in Table 3 show that in the process of leaching lepidolite with hydrochloric acid, enhanced stirring cannot significantly improve the leaching efficiency of Li in the late stages of the reaction. When the temperature is below 373 K, hydrochloric acid does not volatilize in large quantities. Therefore, in this temperature region, increasing the temperature can increase the leaching efficiency of Li.

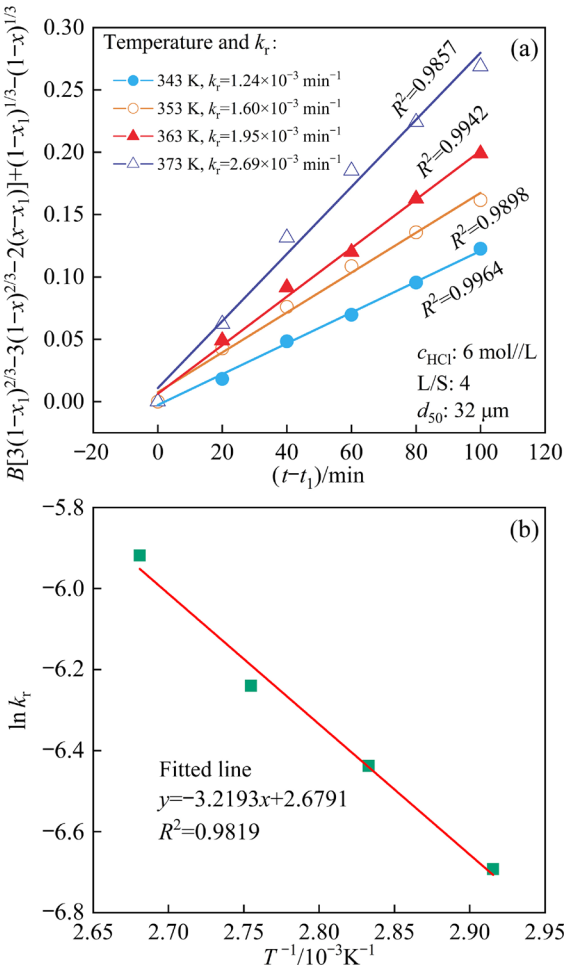

Fig. 6 (a) Plot of $B[3(1-x_1)^{2/3}-3(1-x)^{2/3}-2(x-x_1)]+(1-x_1)^{1/3}-(1-x)^{1/3}$ vs $(t-t_1)$ at different temperatures within 0−120 min; (b) Arrhenius plot for Li leaching

3.5 Economic estimation of leaching neutralization process

According to our previous reports [26], the evaporation−concentration and crystallization−calcination processes can recover nearly 70% of the residual hydrochloric acid in the leaching solution, reducing the cost of neutralizing the residual acid before precipitating Li_2CO_3. In addition, the product value, raw material cost and processing cost are calculated based on the market price of energy, water and material and the power consumption of the factory equipment. The economic estimation results in Fig. 7 show that leaching lepidolite with hydrochloric acid is more economical than sulfuric acid. Although sulfuric acid can slightly increase the leaching efficiency of Li from lepidolite, the processing cost is high due to the higher temperature and longer time for leaching process [34].

The concentration of Li in the leaching solution is 6.86 g/L (Table 4). Unlike other alkali metal elements, the high concentrations of Ca, Al, F and Si in the solution significantly reduce the purity of the Li_2CO_3 product. Therefore, NaOH solution is used to remove Ca, Al, F and Si. The results show that the concentrations of Ca, Al, F and Si are reduced, but the main non-alkali metal impurity is Ca with a concentration of 0.141 g/L (Table 4). Due to the difference in solubility between Li_2CO_3 and $CaCO_3$, most of Ca in the solution can be removed by adding Na_2CO_3 in two stages [25]. The abnormal increase in

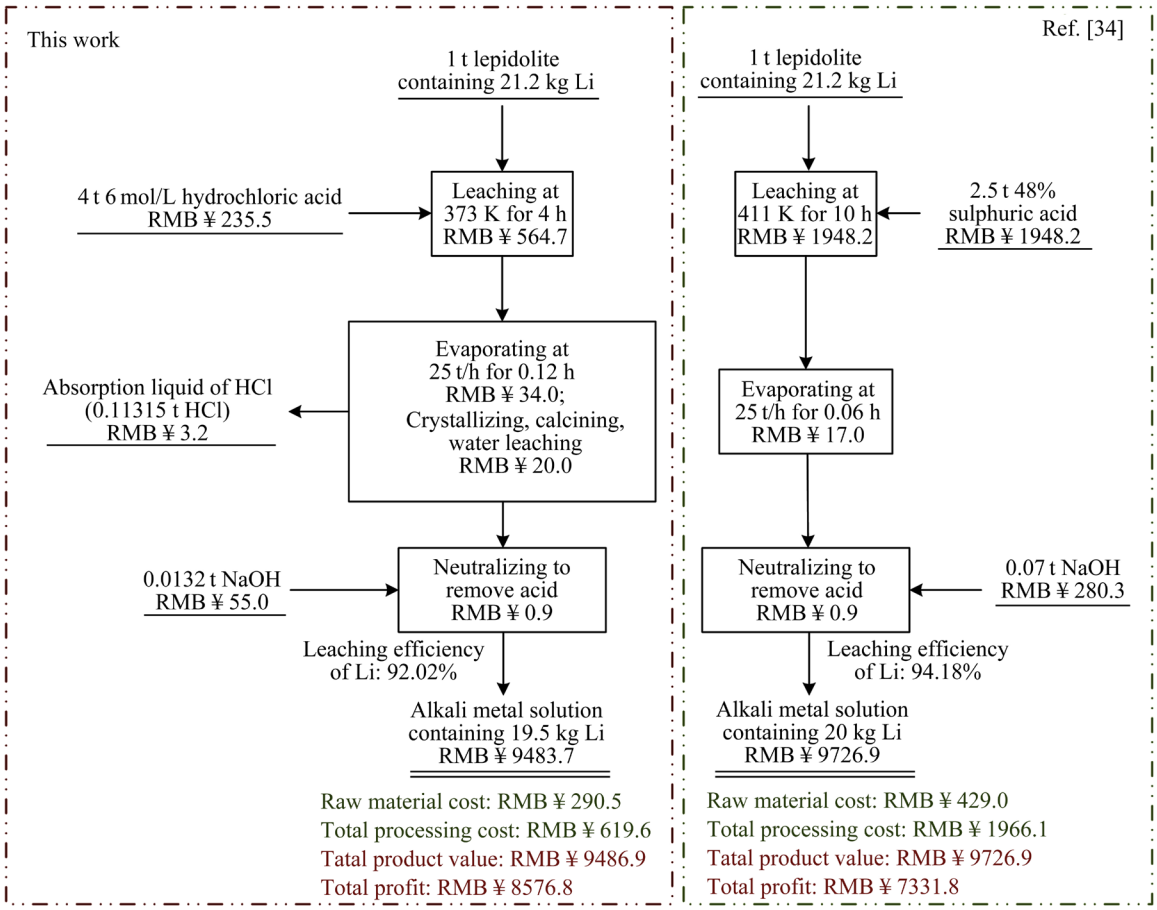

Fig. 7 Comparison of economic estimation results between this work and sulfuric acid leaching for lepidolite [34]

Table 4 Element concentrations in leaching solution and purified solutions (g/L)

Sample	Li	Na	K	Rb	Cs	Al	F	Si	Ca
Solution-1	6.86	2.09	18.72	3.02	0.54	33.26	13.19	0.11	0.630
Solution-2	–	–	–	–	–	0.033	0.032	0.026	0.141
Solution-3	8.87	11.7	25.85	2.49	0.52	0.012	0.054	0.025	0.010

Solution-1 is the leaching solution, solution-2 is the filtrate after neutralizing and impurity removal, and solution-3 is the solution after Ca removal

sodium in the solution is due to the addition of the NaOH solution as a neutralizing agent as well as impurity remover. Under experimental conditions (see Sections 2.2.2 and 2.2.3 for more details), the removal efficiency of Ca and the loss rate of Li are 98.79% and 0.59%, respectively. The impurity contents of Li_2CO_3 synthesized by the precipitation reaction between the solution after Ca removal and the Na_2CO_3 solution are shown in Table 5. It shows that Li_2CO_3 with a purity of 99.89% is prepared from lepidolite through hydrochloric acid leaching and multi-step purification.

Table 5 Impurity contents in Li_2CO_3 with purity of 99.89% (10^{-6})

Na	K	Ca	Mg	Fe	Zn	Cu	Si	Al	Mn	F	S	Cl
56	11	12	1	2	3	1	4	8	2	42	9	23

4 Conclusions

(1) The normal pressure leaching process of lepidolite by hydrochloric acid was systematically studied. The process conditions, including leaching time (4 h), temperature (373 K), initial hydrochloric acid concentration (6 mol/L), L/S (4) and mineral particle size d_{50} (32 μm) for the leaching process are optimized. Under these conditions, leaching efficiencies of Li, K, Rb, Cs and Al are 92.02%, 93.31%, 88.59%, 86.75% and 81.07%, respectively.

(2) The leaching process conforms to the shrinking core model. At a particular stage, the leaching process is under mixed control of chemical reactions and diffusion through the solid product layer of the associated minerals.

(3) As the temperature increases, the contribution of solid product layer diffusion to the leaching gradually expands, but it is still significantly less than the contribution of chemical reactions.

(4) Cost savings in neutralizing agents and leaching processes make hydrochloric acid a more economical leaching agent than sulfuric acid for lepidolite. Li_2CO_3, with a purity of 99.89%, is synthesized from the hydrochloric acid leachate.

CRediT authorship contribution statement

Song-lin LIU: Methodology, Date curation, Investigation, Writing – Original draft; **Jin-lian LIU:** Methodology, Date curation, Investigation; **Xiao-peng SONG:** Supervision, Funding acquisition; **Zhou-lan YIN:** Supervision, Funding acquisition; **Xin-hai LI:** Supervision, Funding acquisition; **Zhi-xing WANG:** Supervision, Funding acquisition; **Hua-jun GUO:** Supervision, Funding acquisition; **Guo-chun YAN:** Supervision, Funding acquisition; **Qi-yang HU:** Supervision, Funding acquisition; **Xun-hui XIONG:** Supervision, Funding acquisition; **Jie-xi WANG:** Conceptualization, Supervision, Writing – Review & editing, Funding acquisition.

Declaration of competing interest

The authors declare that they have no known competing financial interests or personal relationships that could have appeared to influence the work reported in this paper.

Acknowledgments

This work was supported by the National Natural Science Foundation of China (No. 52122407), the National Key Research & Development Program of China (No. 2022YF2906200), and the Science and Technology Innovation Program of Hunan Province, China (No. 2022RC3048). We also thank Jiangxi Yunwei New Materials Co., Ltd., China, for resource and financial support.

References

[1] FRITH J T, LACEY M J, ULISSI U. A non-academic perspective on the future of lithium-based batteries [J]. Nature Communications, 2023, 14(1): 420.

[2] CAO Ning, ZHANG Ya-li, CHEN Lin-lin, JIA Yun, HUANG Yao-guo. Priority recovery of lithium and effective leaching of nickel and cobalt from spent lithium-ion battery [J]. Transactions of Nonferrous Metals Society of China, 2022, 32(5): 1677−1690.

[3] GARCIA L V, HO Y C, MYO THANT M M, HAN D S, LIM J W. Lithium in a sustainable circular economy: A comprehensive review [J]. Processes, 2023, 11: 418.

[4] YU Zhen, WANG Yi-lan, MA Xiao-qian, SHUAI Chuan-min, ZHAO Yu-jia. How critical mineral supply security affects China NEVs industry? Based on a prediction for chromium and cobalt in 2030 [J]. Resources Policy, 2023, 85: 103861.

[5] LIU Dong-hui, GAO Xiang-yun, AN Hai-zhong, QI Ya-bin, SUN Xiao-qi, WANG Ze, CHEN Zhi-hua, AN Feng, JIA Nan-fei. Supply and demand response trends of lithium resources driven by the demand of emerging renewable energy technologies in China [J]. Resources, Conservation and Recycling, 2019, 145: 311−321.

[6] CHEN Wu, SUN Xin, LIU Li-tao, LIU Xiao-jie, ZHANG Rui, ZHANG Shao-hui, XUE Jin-jun, SUN Qian, WANG Min-xi, LI Xin, YANG Jian-xin, HERTWICH E, GE Quan-sheng, LIU Gang. Carbon neutrality of China's passenger car sector requires coordinated short-term behavioral changes and long-term technological solutions [J]. One Earth, 2022, 5(8): 875−891.

[7] BATTISTEL A, PALAGONIA M S, BROGIOLI D, LA MANTIA F, TRÓCOLI R. Electrochemical methods for lithium recovery: A comprehensive and critical review [J]. Advanced Materials, 2020, 32(23): e1905440.

[8] CHANG Xin, FAN Min, YUAN Bo-heng, GU Chao-fan, HE Wei-huan, LI Chen, FENG Xi-xi, XIN Sen, MENG Qing-hai, WAN Li-jun, GUO Yu-guo. Potential controllable redox couple for mild and efficient lithium recovery from spent batteries [J]. Angewandte Chemie International Edition, 2023, 62(41): e202310435.

[9] XIE Rui-qi, ZHAO Zhi-hui, TONG Xiong, XIE Xian, SONG Qiang, FAN Pei-qiang. Review of the research on the development and utilization of clay-type lithium resources [J]. Particuology, 2024, 87: 46−53.

[10] BISHIMBAYEVA G, ZHUMABAYEVA D, ZHANDAYEV N, NALIBAYEVA A, SHESTAKOV K, LEVANEVSKY I, ZHANABAYEVA A. Technological improvement lithium recovery methods from primary resources [J]. Oriental Journal of Chemistry, 2018, 34(6): 2762−2769.

[11] ZHANG Shi-yu, JIANG Yu-rong, YUE Xiao-lin, ZHANG Run-nan, LI Run-lai, GU Tian-run, WU Tao, ZHAO Jun-hui, ZHANG Sui, JIANG Zhong-yi. Bifunctional polyhedral oligomeric silsesquioxane engineered polyamide membrane for efficient Li^+/Mg^{2+} separation [J]. Separation and Purification Technology, 2023, 327: 124875.

[12] FU Lin, HU Yu-hao, LIN Xiang-bin, WANG Qing-chen, YANG Lin-sen, XIN Wei-wen, ZHOU Sheng-yang, QIAN Yong-chao, KONG Xiang-yu, JIANG Lei, WEN Li-ping. Engineering multi-field-coupled synergistic ion transport system based on the heterogeneous nanofluidic membrane for high-efficient lithium extraction [J]. Nano-Micro Letters, 2023, 15(1): 130.

[13] DESSEMOND C, LAJOIE-LEROUX F, SOUCY G, LAROCHE N, MAGNAN J F. Spodumene: The lithium market, resources and processes [J]. Minerals, 2019, 9(6): 334.

[14] LIU Chong, LI Yan-bin, LIN Ding-chang, HSU P C, LIU Bo-fei, YAN Gang-bin, WU Tong, CUI Yi, CHU S. Lithium extraction from seawater through pulsed electrochemical intercalation [J]. Joule, 2020, 4(7): 1459−1469.

[15] RESENTERA A C, ROSALES G D, ESQUIVEL M R, RODRIGUEZ M H. Thermal and structural analysis of the reaction pathways of α-spodumene with NH_4HF_2 [J]. Thermochimica Acta, 2020, 689: 178609.

[16] YAN Qun-xuan, LI Xin-hai, YIN Zhou-lan, WANG Zhi-xing, GUO Hua-jun, PENG Wen-jie, HU Qi-yang. A novel process for extracting lithium from lepidolite [J]. Hydrometallurgy, 2012, 121/122/123/124: 54−59.

[17] VIECELI N, A. NOGUEIRA C A, PEREIRA M F C, DURÃO F O, GUIMARÃES C, MARGARIDO F. Recovery of lithium carbonate by acid digestion and hydrometallurgical processing from mechanically activated lepidolite [J]. Hydrometallurgy, 2018, 175: 1−10.

[18] SIAME E, PASCOE R D. Extraction of lithium from micaceous waste from China clay production [J]. Minerals Engineering, 2011, 24(14): 1595−1602.

[19] XING Peng, WANG Cheng-yan, CHEN Yong-qiang, MA Bao-zhong. Rubidium extraction from mineral and brine resources: A review [J]. Hydrometallurgy, 2021, 203: 105644.

[20] VU H, BERNARDI J, JANDOVÁ J, VACULÍKOVÁ L, GOLIÁŠ V. Lithium and rubidium extraction from zinnwaldite by alkali digestion process: Sintering mechanism and leaching kinetics [J]. International Journal of Mineral Processing, 2013, 123: 9−17.

[21] CHOUBEY P K, KIM M S, SRIVASTAVA R R, LEE J C, LEE J Y. Advance review on the exploitation of the prominent energy-storage element: Lithium. Part I: From mineral and brine resources [J]. Minerals Engineering, 2016, 89: 119−137.

[22] LIU Jin-lian, YIN Zhou-lan, LI Xin-hai, HU Qi-yang, LIU Wei. A novel process for the selective precipitation of valuable metals from lepidolite [J]. Minerals Engineering, 2019, 135: 29−36.

[23] WANG Ya-hui, WU Ji-jun, HU Guo-chen, MA Wen-hui. Recovery of Li and Fe from spent lithium iron phosphate using organic acid leaching system [J]. Transactions of Nonferrous Metals Society of China, 2024, 34(1): 336−346.

[24] YAN Qun-xuan, LI Xin-hai, WANG Zhi-xing, WU Xi-fei, WANG Jie-xi, GUO Hua-jun, HU Qi-yang, PENG Wen-jie. Extraction of lithium from lepidolite by sulfation roasting and water leaching [J]. International Journal of Mineral Processing, 2012, 110/111: 1−5.

[25] YAN Qun-xuan, LI Xin-hai, WANG Zhi-xing, WU Xi-fei, GUO Hua-jun, HU Qi-yang, PENG Wen-jie, WANG Jie-xi. Extraction of valuable metals from lepidolite [J]. Hydrometallurgy, 2012, 117/118: 116−118.

[26] LIU Jin-lian, YIN Zhou-lan, LIU Wei, LI Xin-hai, HU Qi-yang. Treatment of aluminum and fluoride during hydrochloric acid leaching of lepidolite [J]. Hydrometallurgy, 2020, 191: 105222.

[27] LI Y, KAWASHIMA N, LI J, CHANDRA A P, GERSON A R. A review of the structure, and fundamental mechanisms and kinetics of the leaching of chalcopyrite [J]. Advances in Colloid and Interface Science, 2013, 197/198: 1−32.

[28] RIOYO J, TUSET S, GRAU R. Lithium extraction from spodumene by the traditional sulfuric acid process: A review [J]. Mineral Processing and Extractive Metallurgy Review, 2022, 43(1): 97−106.

[29] STERBA J, KRZEMIEŃ A, RIESGO FERNÁNDEZ P, ESCANCIANO GARCÍA-MIRANDA C, FIDALGO VALVERDE G. Lithium mining: Accelerating the transition to sustainable energy [J]. Resources Policy, 2019, 62: 416−426.

[30] GREIM P, SOLOMON A A, BREYER C. Assessment of lithium criticality in the global energy transition and addressing policy gaps in transportation [J]. Nature Communications, 2020, 11(1): 4570.

[31] GU Han-nian, GUO Teng-fei, WEN Han-jie, LUO Chong-guang, CUI Yi, DU Sheng-jiang, WANG Ning. Leaching efficiency of sulfuric acid on selective lithium leachability from bauxitic claystone [J]. Minerals Engineering, 2020, 145: 106076.

[32] WANG Hai-dong, ZHOU An-an, GUO Hui, LÜ Meng-hua, YU Hai-zhao. Kinetics of leaching lithium from lepidolite using mixture of hydrofluoric and sulfuric acid [J]. Journal of Central South University, 2020, 27(1): 27−36.

[33] DING Wei, BAO Shen-xu, ZHANG Yi-min, XIAO Jun-hui. Mechanism and kinetics study on ultrasound assisted leaching of gallium and zinc from corundum flue dust [J]. Minerals Engineering, 2022, 183: 107624.

[34] LIU Jin-lian, YIN Zhou-lan, LI Xin-hai, HU Qi-yang, LIU Wei. Recovery of valuable metals from lepidolite by atmosphere leaching and kinetics on dissolution of lithium [J]. Transactions of Nonferrous Metals Society of China, 2019, 29(3): 641−649.

[35] YAN Qun-xuan, LI Xin-hai, WANG Zhi-xing, WANG Jie-xi, GUO Hua-jun, HU Qi-yang, PENG Wen-jie, WU Xi-fei. Extraction of lithium from lepidolite using chlorination roasting–water leaching process [J]. Transactions of Nonferrous Metals Society of China, 2012, 22(7): 1753−1759.

[36] GAO Ya, YUE Tong, SUN Wei, HE Dong-dong, LU Cheng-long, FU Xin-zhuang. Acid recovering and iron recycling from pickling waste acid by extraction and spray pyrolysis techniques [J]. Journal of Cleaner Production, 2021, 312: 127747.
[37] XIAO Jie-feng, NIU Bo, SONG Qing-ming, ZHAN Lu, XU Zhen-ming. Novel targetedly extracting lithium: An environmental-friendly controlled chlorinating technology and mechanism of spent lithium ion batteries recovery [J]. Journal of Hazardous Materials, 2021, 404: 123947.
[38] LI Min-ting, WEI Chang, QIU Shuang, ZHOU Xue-jiao, LI Cun-xiong, DENG Zhi-gan. Kinetics of vanadium dissolution from black shale in pressure acid leaching [J]. Hydrometallurgy, 2010, 104(2): 193−200.
[39] SALAKJANI N K, SINGH P, NIKOLOSKI A N. Production of lithium — A literature review (part 1): Pretreatment of spodumene [J]. Mineral Processing and Extractive Metallurgy Review, 2019, 41(5): 335−348.
[40] XU Ying-peng, LIU Xu-heng, ZHAO Zhong-wei, CHEN Xing-yu, LI Jiang-tao, HE Li-hua, SUN Feng-long. Kinetics and mechanism of selective leaching of bismuth from molybdenite and bismuthinite mixed ore [J]. Hydrometallurgy, 2024: 224.
[41] QU Li-li, HE Ya-qun, FU Yuan-peng, XIE Wei-ning, YE Cui-ling, LU Qi-chang, LI Jin-long, LI Jia-hao, PANG Zhi-bo. Enhancement of leaching of cobalt and lithium from spent lithium-ion batteries by mechanochemical process [J]. Transactions of Nonferrous Metals Society of China, 2022, 32(4): 1325−1335.
[42] GUO Hui, KUANG Ge, WAN Hao, YANG Yi, YU Hai-zhao, WANG Hai-dong. Enhanced acid treatment to extract lithium from lepidolite with a fluorine-based chemical method [J]. Hydrometallurgy, 2019, 183: 9−19.
[43] FARAJI F, ALIZADEH A, RASHCHI F, MOSTOUFI N. Kinetics of leaching: A review [J]. Reviews in Chemical Engineering, 2022, 38(2): 113−148.
[44] LI Wei-lun, CHEN Yong-ming, LI Shuai, WANG Chang-hong, LI Yun, ZHAO Tian-yu, TRAVERSY M, CHANG Cong, JIE Ya-fei, HE Jing, TANG Chao-bo, YANG Sheng-hai. Leaching kinetics of de-lithium residue from spent ternary lithium-ion battery cathodic materials with starch as reductant [J]. Transactions of Nonferrous Metals Society of China, 2023, 33(2): 619−631.
[45] NAZEMI M K, RASHCHI F, MOSTOUFI N. A new approach for identifying the rate controlling step applied to the leaching of nickel from spent catalyst [J]. International Journal of Mineral Processing, 2011, 100(1/2): 21−26.
[46] LI Li, BIAN Yi-fan, ZHANG Xiao-xiao, GUAN Yi-biao, FAN Er-sha, WU Feng, CHEN Ren-jie. Process for recycling mixed-cathode materials from spent lithium-ion batteries and kinetics of leaching [J]. Waste Manag, 2018, 71: 362−371.
[47] LAMPINEN M, SEISKO S, FORSSTRÖM O, LAARI A, AROMAA J, LUNDSTRÖM M, KOIRANEN T. Mechanism and kinetics of gold leaching by cupric chloride [J]. Hydrometallurgy, 2017, 169: 103−111.
[48] TAN Quan-yin, DENG Chao, LI Jin-hui. Effects of mechanical activation on the kinetics of terbium leaching from waste phosphors using hydrochloric acid [J]. Journal of Rare Earths, 2017, 35(4): 398−405.
[49] AARABI-KARASGANI M, RASHCHI F, MOSTOUFI N, VAHIDI E. Leaching of vanadium from LD converter slag using sulfuric acid [J]. Hydrometallurgy, 2010, 102(1/2/3/4): 14−21.
[50] BOBECK G E, SU H. The kinetics of dissolution of sphalerite in ferric chloride solution [J]. Metallurgical Transactions B, 1985, 16: 413−424.
[51] KARIMI S, RASHCHI F, MOGHADDAM J. Parameters optimization and kinetics of direct atmospheric leaching of Angouran sphalerite [J]. International Journal of Mineral Processing, 2017, 162: 58−68.

锂云母中有价金属的盐酸浸出及锂浸出动力学

刘松霖[1]，刘金练[1,2]，宋小鹏[3]，尹周澜[2]，李新海[1,4]，王志兴[1,4]，郭华军[1,4]，
颜果春[1,4]，胡启阳[1,3]，熊训辉[5]，王接喜[1,3,4]

1. 中南大学 冶金与环境学院，长沙 410083；
2. 中南大学 化学化工学院，长沙 410083；
3. 江西云威新材料股份有限公司，宜春 330700；
4. 国家先进储能材料工程技术研究中心，长沙 410205；
5. 华南理工大学 环境与能源学院，广州 510006

摘　要：系统探讨了锂云母在盐酸中的浸出过程及其动力学行为。研究了浸出条件对锂云母中有价元素浸出效率的影响。在最佳浸出条件下，Li、K、Rb、Cs 和 Al 的浸出率分别为 92.02%、93.31%、88.59%、86.75%和 81.07%。动力学研究结果表明，浸出过程符合由化学反应与固体产物层扩散混合控制的收缩核模型；另外，随着温度的升高，固体产物层扩散对浸出的影响逐渐扩大，但仍明显小于化学反应的影响。中和剂和浸出条件上的成本节约使盐酸成为一种经济的锂云母浸出剂。最后，用盐酸浸出液合成了纯度为 99.89%的 Li_2CO_3。

关键词：锂云母；锂提取；盐酸浸出；动力学

(Edited by Wei-ping CHEN)